SOIL MOISTURE AND REMOTELY SENSED SPECTRAL DATA IN A PARTIAL CANOPY COTTON FIELD AT THE MARICOPA AGRICULTURAL CENTER, PINAL COUNTY, ARIZONA, 1988

By SANDRA J. OWEN-JOYCE

U.S. GEOLOGICAL SURVEY
Water-Resources Investigations Report 92—4133

Prepared in cooperation with the
ARIZONA DEPARTMENT OF WATER RESOURCES

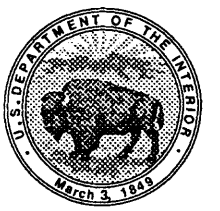

Tucson, Arizona
November 1992

U.S. DEPARTMENT OF THE INTERIOR
MANUEL LUJAN, Jr., Secretary

U.S. GEOLOGICAL SURVEY
Dallas L. Peck, Director

For additional information
write to:

District Chief
U.S. Geological Survey
Water Resources Division
375 South Euclid Avenue
Tucson, Arizona 85719

Copies of this report can be
purchased from:

U.S. Geological Survey
Books and Open-File Reports Section
Federal Center
Box 25425
Denver, Colorado 80225

CONTENTS

ILLUSTRATIONS

CONTENTS

CONTENTS

TABLES

CONVERSION FACTORS

Multiply	*By*	*To obtain*
Area		
square meter (m^2)	10.76	square foot (ft^2)
hectare (ha)	2.471	acre
Length		
kilometer (km)	0.621	mile (m)
meter (m)	3.281	foot (ft)
centimeter (cm)	0.3937	inch (in.)
micrometer (μm)	3.937×10^{-5}	inch (in.)
Power		
watt (W)	3.412	British thermal units per hour (Btu/h)
	0.2388	calories per second (cal/s)
Pressure		
kilopascal (kPa)	0.2953	inches of mercury (in. Hg)
	0.1450	pound per square inch (lb/in^2)
	10	millibar (mbar)
bar	1.0×10^5	pascals (Pa)
	0.9869	atmosphere (Atm)
	14.5030	pounds per square inch (lb/in^2)
Temperature		
degree Celsius (°C)	°F = 1.8 × °C + 32	degree Fahrenheit (°F)
Volume		
cubic meter (m^3)	8.107×10^{-4}	acre-foot (acre-ft)

SOIL MOISTURE AND REMOTELY SENSED SPECTRAL DATA IN A PARTIAL CANOPY COTTON FIELD AT THE MARICOPA AGRICULTURAL CENTER, PINAL COUNTY, ARIZONA, 1988

By

Sandra J. Owen-Joyce

ABSTRACT

Gravimetric soil-moisture contents, remotely sensed spectral data obtained from an aircraft platform, and ground-based meteorological data were collected to investigate how closely the spatial distribution of latent heat flux density corresponded to variations in soil moisture. Data were collected at the University of Arizona Maricopa Agricultural Center in June 1988.

Surface soils in the dry part of the field showed a slight temporal trend in soil moisture associated with groups of furrows irrigated at different times. Soil moisture did not vary as a function of soil texture or surface roughness. Surface temperature is the remotely sensed component of the remote method of estimating evapotranspiration, but under partial-canopy conditions, surface temperature is a composite of the plants, soil, and shaded surfaces within the sensor field of view. During June 1988, the hot soil surface dominated the composite surface temperature in the partial canopy cotton field. Changes in surface temperature correlated with changes in surface roughness and soil moisture. Changes in soil surface masked any change caused by differences in ground cover.

Geographic information system (GIS) software was used to compare the ground-based measurements of soil moisture to remotely sensed data. A rigorous comparison of spatial data sets with GIS is limited by the inaccuracies in the positioning of spatial data points, which transfer directly into any spatial comparisons and result in a misrepresentation of relations between mapped variables. Improvements in determining the ground position of the data collected from an aircraft are required to enhance the use of aircraft data in a GIS analysis.

INTRODUCTION

Cooperative research studies of evapotranspiration (ET), organized by the U.S. Department of Agriculture, Agricultural Research Service, Water Conservation Laboratory, began in April 1985 at the University of Arizona (UA) Maricopa Agricultural Center (MAC) (fig. 1).

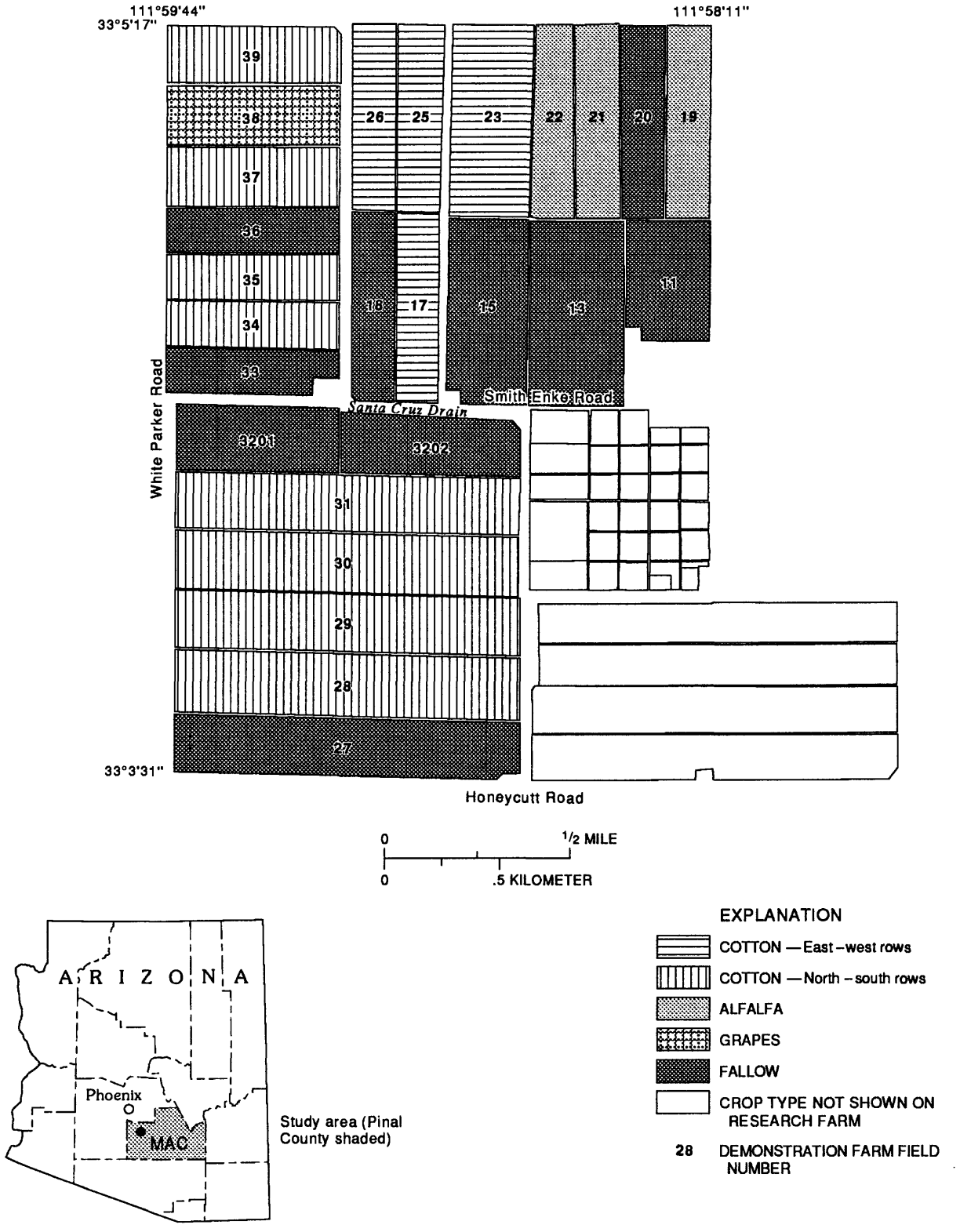

Figure 1.—Location of the Maricopa Agricultural Center (MAC), Pinal County, Arizona, and crop types on June 11-13, 1988.

MAC experiments vary in length and include participation by scientists of the U.S. Geological Survey (USGS) and other agencies who share the data collected (Moran, 1986a, 1986b). The third MAC experiment, June 11-13, 1988, included this project as one of many individual efforts to collect the ancillary data necessary to explore the relation between the spatial distribution of ET and the variables that affect it. Extensive field measurements were made in conjunction with three satellite overpasses.

Preliminary results from earlier MAC experiments indicated that under clear sky conditions and over uniformly cropped fields (1) ET can be calculated by using remotely sensed data and compared closely with ET measured continuously on the ground using a Bowen ratio system (Raymond and others, 1988) and (2) the spatial distribution of ET corresponded more closely to elapsed time since the most recent irrigation than to crop type, soil type, or vegetation density in a cropped field (Raymond and others, 1987). Work begun in the second MAC experiment to apply the remote method of ET estimation over nonuniform surface conditions was continued during the third experiment over partial canopy cotton. The objective of this project was to map the spatial distribution of ET in relation to soil moisture. This paper presents (1) the data collected to investigate the relation between gravimetric soil moisture and remotely sensed surface temperature and (2) a discussion regarding the problems encountered attempting to meet the objective to investigate the relation between gravimetric soil moisture and ET estimated using the method developed by Jackson and others (1987) for use with remotely sensed data.

Approach

The spatial distribution of ET was calculated using an energy budget with remotely sensed visible, near-infrared, and thermal radiation data from aircraft. Instantaneous and daily ET data were provided by M. Susan Moran and Ray D. Jackson, U.S. Department of Agriculture, Water Conservation Laboratory, Phoenix, Arizona.

The spatial and temporal distribution of available soil moisture and soil-water content was measured using gravimetric methods in a cotton field at MAC. The soil-moisture studies were conducted over a 2- to 3-week period to include preirrigation conditions prior to the satellite overpasses, during the time of the overpasses to relate available soil moisture to ET rates, and about 1 week after the overpasses to determine soil moisture depletion rates at selected locations. Soil moisture, particle-size distribution, and moisture-retention data were collected by Arthur W. Warrick and colleagues, University of Arizona, Department of Soil and Water Science, under contract to the USGS.

Maps comparing the spatial data were prepared by the USGS. The ARC/INFO[1] geographic information system (GIS) software was used to compare two types of spatial-data sets—remotely sensed data and ground-based soil-moisture data. The software translates mapped data into digital form and stores the data as coverages. In a previous study, use of ARC/INFO allowed spatial

[1]Use of the brand name in this report is for identification purposes only and does not constitute endorsement by the U.S. Geological Survey.

variables to be directly compared regardless of format, resolution, or relative location (Raymond and others, 1987). Transfer of coverages between participating scientists proved easy and useful in preventing duplication of work. Maps were generated using ARC/INFO GIS software. The project was done in cooperation with the Arizona Department of Water Resources.

Acknowledgments

The author wishes to acknowledge the continuing support and cooperation of the personnel at the Maricopa Agricultural Center. M. Susan Moran and Ray D. Jackson, U.S. Water Conservation Laboratory, provided answers to many questions and helped test some suggested changes to their methodology. Thanks to David S. Ammon, Aerial Images, whose innovative instrument designs and flying skills made collection of the aircraft data possible. John J. Regan, University of Arizona, provided copies of the ARC covers of the surveyed field boundaries and of soil types and textures.

DESCRIPTION OF THE STUDY AREA

MAC is a 770-ha research and demonstration farm about 48 km south of Phoenix (fig. 1) owned by the University of Arizona. MAC experiments are set up mainly on the demonstration farm, which includes fields 11 to 39; fields on the research farm are unnumbered on the map. The distribution of crops by type on the demonstration farm for June 1988 is shown in figure 1. Field boundaries were surveyed by the UA (Regan and others, 1989) and an ARC cover was created. The UA field-boundary map is more accurate than the previous USGS version digitized from an aerial photograph because the increased resolution allows the roads to be separated from the individual fields. Points surveyed were tied to the locations for which Universal Transverse Mercator (UTM) coordinates were known—section and half-section corners on the farm. All point data were reported in UTM meters. A copy of the ARC cover with the surveyed field boundaries was obtained for use in this study (John J. Regan, Computer Applications Specialist, University of Arizona, written commun., 1988).

Crop Data

In June 1988, field 28 (38.4 ha) was an area of intense data collection by experiment participants. Field 28 was planted with cotton (*Gossypium hirsutum* L., variety DPL-77) in north-south rows on day 89 (March 29). Plant density during the experiment was 11.8 plants/m^2 and plant height was about 31 cm; percentage of ground cover was about 20 percent. About 4 ha in the middle of the field just west of center were replanted April 14. This area included Paul Pinter's (Research Biologist, U.S. Water Conservation Laboratory, written commun., 1988) data-collection site B, but exact boundaries are unknown. Plant density in the replanted section was 7.7 plants/m^2 and plant height was about 21 cm; percentage of ground cover was about 11 percent (Daughtry and others, 1990, table 2).

Soil Types and Textures

UA field studies at MAC characterized the soils and produced a soil-type map and a soil-texture map (Post and others, 1988). ARC coverages of the soil types and soil textures were created at the UA and copies were obtained for use in this study (John J. Regan, Computer Applications Specialist, University of Arizona, written commun., 1988). Data were extracted from the MAC ARC coverages and new coverages were created that contained only the data for field 28 (fig. 2). All the soils on the farm have been reclaimed because of land-leveling and soil-reclamation activities related to agricultural development and are so noted (Post and others, 1988). Soils on field 28 are composed of the Trix-Casa Grande association, reclaimed, in the west half; Trix soil series, reclaimed, in the east half; and Casa Grande soil series, reclaimed, in the extreme northeast corner (fig. 2). The textures of the surface horizons (0-30 cm depth) on field 28 are sandy loam, sandy clay loam, and clay loam (Post and others, 1988). Most of the field is clay loam except west of the center, where an area of sandy loam is bordered by sandy clay loam.

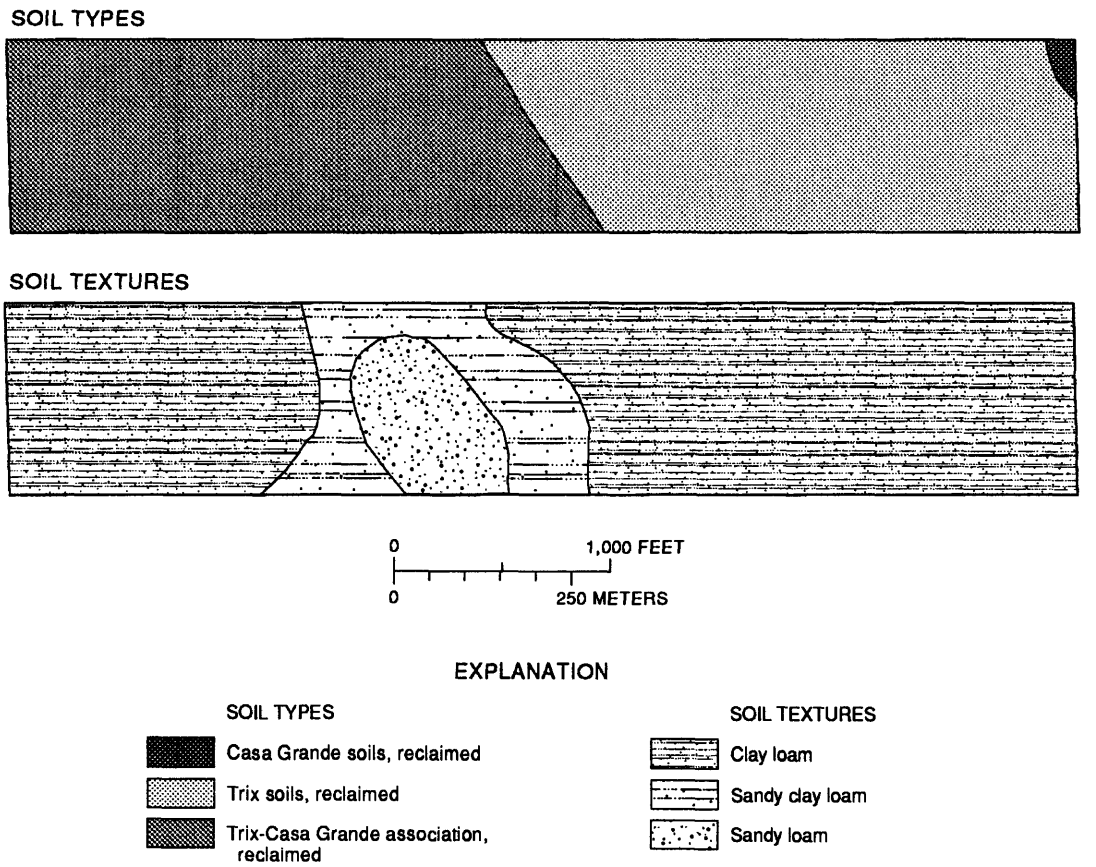

Figure 2.—Soil types and textures (0–30 centimeters depth) in field 28 at the Maricopa Agricultural Center (mapped by Post and others, 1988).

SOIL MOISTURE

Field 28 was irrigated beginning on day 153 (June 1). The field was irrigated from east to west, which took about 5 days (A. Pat Murphree, MAC, oral commun., 1989) because groups of furrows are flood irrigated, one group at a time, from a canal along the south field boundary. During this irrigation, 1,645 m^3/ha was applied. The pattern of irrigation causes soil moisture to vary temporally as well as spatially.

Soil samples were collected during the morning hours of day 164 (June 12) at 45 fixed sampling sites on a 100- × 100-m grid and at 46 "random" sites (fig. 3). The fixed sampling sites lie along three east-west rows 50 m, 150 m, and 250 m north of the south boundary of field 28 (fig. 3). Gravimetric soil-moisture contents were determined at depths of 0-5, 5-15, and 20-30 cm. Supporting data included particle-size distribution and moisture retention at 0.33, 1, and 15 bars of tension. Soil-moisture data also were collected on day 152 (May 31) to determine preirrigation conditions. Analysis of the data by Huete and Warrick (1990) showed strong spatial variability and a well-defined spatial gradient in water content at all three sampling depths.

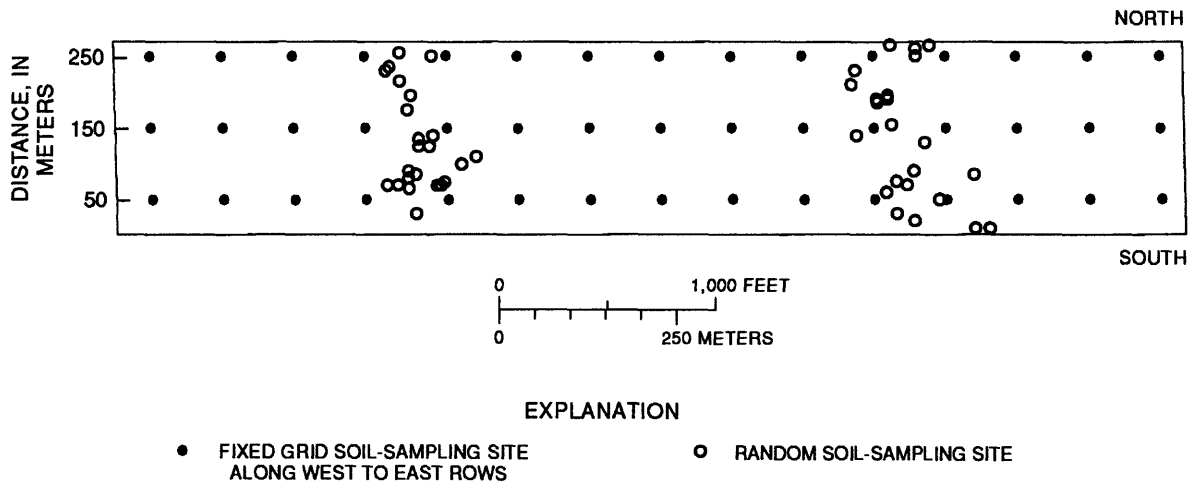

Figure 3.—Location of the soil-sampling sites in field 28 at the Maricopa Agricultural Center.

Soil-moisture content for the upper 5 cm of soil on day 164 was plotted against preirrigation moisture content on day 152 along the three east-west rows of sampling sites (fig. 4). On day 164, a significant change in soil moisture occurred 400 m east of the west boundary of field 28 because of irrigation. The west 400 m of the field were wet, soil moisture increased from about 14 percent in the south to about 24 percent in the north. The east 1,100 m of field 28 were dry (less than 12 percent); moisture content on day 164 generally was at or near the preirrigation levels in the top 0-5 cm. Soil moisture most closely approximated preirrigation levels along the southernmost row (50 m north of the south boundary). The dry area had a smooth and cracked surface except for the easternmost 260 m, which was cultivated. In the smooth area from about 700 to 1,100 m east of

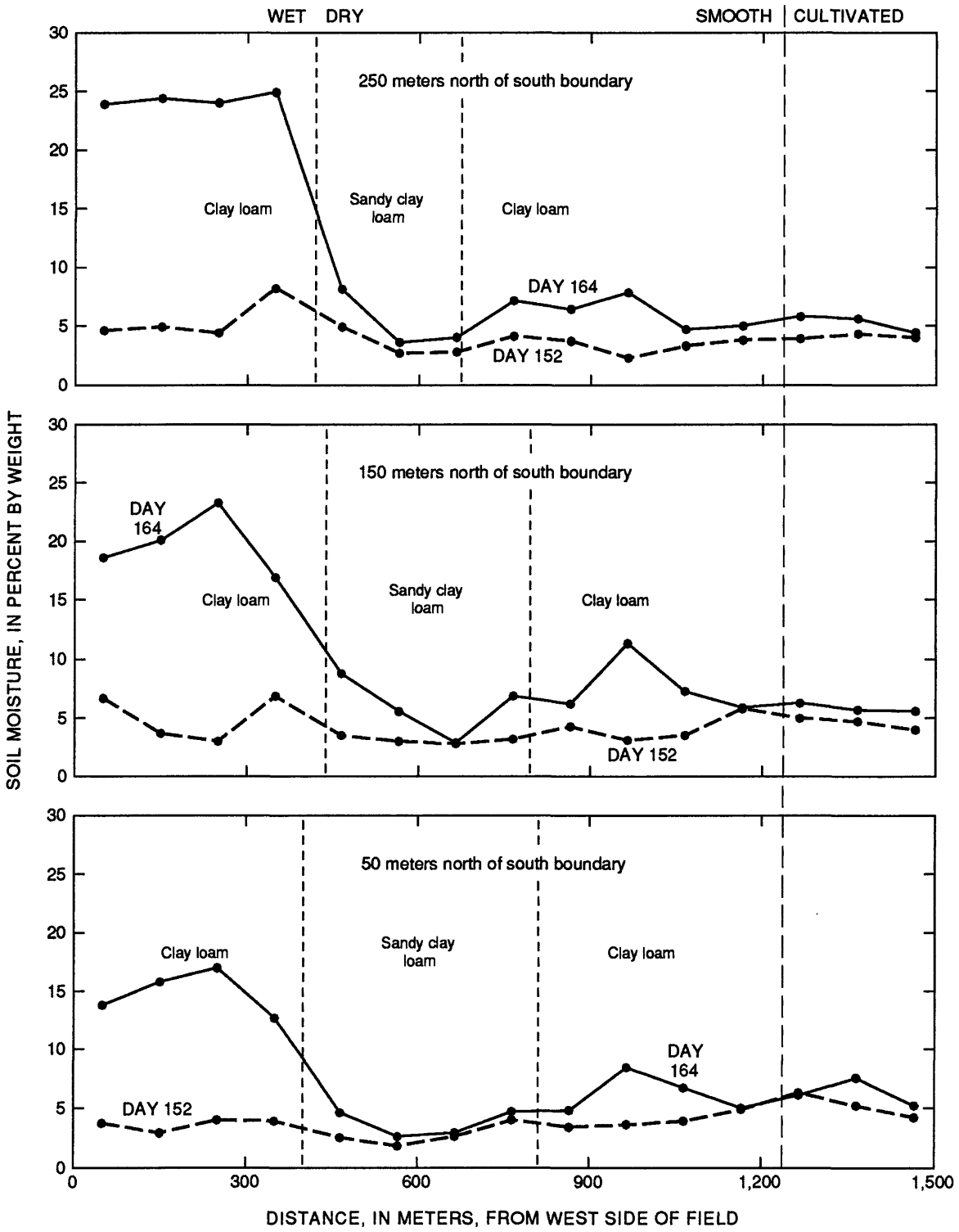

Figure 4.—Soil moisture (0-5 centimeters depth) measured along three east-west rows, 250, 150, and 50 meters north of the south boundary of field 28, Maricopa Agricultural Center, on day 152, preirrigation, and on day 164, 7-12 days after irrigation that proceeded from east to west.

the west boundary, the larger difference between moisture content from day 152 to day 164 could be related to that area being irrigated after the area to the east; soil type and texture were the same in both areas.

Changes in surface roughness (smooth or cultivated) do not correlate with any distinctive changes in moisture content. Particle-size data determined for the soil samples at depths of 0-5 cm were plotted along the three east-west rows in field 28 (fig. 5). The particle-size data correspond to the soil textures (0-30 cm depth) mapped by Post and others (1988). The highest percentages of sand occur in an area that varies in width and is centered about 590 to 600 m east of the west side of the field. This area, although irrigated after the area to the east, has lower soil moisture mainly along the rows 50 and 250 m north of the south field boundary. In this area, the low soil moisture probably was caused by the combined effect of less ground cover, and therefore greater bare-soil evaporation, and more rapid percolation because of the higher sand concentration.

Point coverages of the sampling sites, 45 fixed points on a 100- × 100-m grid and 46 random points, were generated using ARC/INFO; the soil-moisture content at each of the three depths was entered as attribute data. Soil-moisture data at the random points were available only on day 164. The data were plotted and hand contoured. The contour lines were digitized and line coverages were built. Although the moisture content was higher at depth, spatial trends were similar for all three sampling depths (fig. 6).

A polygon coverage of zoned soil moisture was built from the line coverage and overlaid on the soil-texture map of field 28 (fig. 7) to spatially investigate any correlation between soil moisture and texture. Soil moisture of less than 4 percent corresponded to the areas with the highest percentage of sand but did not distinguish between sandy loam and sandy clay loam (fig. 7). Soil moisture may not show a relation to soil texture as the two rows closest to the north and south boundaries are the only rows to clearly show a decrease at more than one sampling point, which may be related to edge-effect drying. Contour maps of soil moisture do show higher soil moisture in the central part of the dry area (east 1,100 m of field) at all three sampling depths (fig. 6). The sandy loam also corresponds to the area where the plant density decreased. The lack of a direct relation between soil moisture and soil texture is best illustrated with plots of soil moisture as a function of the percentage of sand and clay measured at the same sampling sites (fig. 8).

Plants continue to transpire water from the root zone, although the soil at the surface is dry. Moisture-retention data at 15 bars of tension (wilting point) measured for each of the fixed sampling sites were compared to the soil moisture measured at the same depth to determine if the plants were under stress. At a depth of 0-5 cm, only the sampling sites at the west side of the field, where soil moisture exceeded about 17 percent, had water available for use by plants. At depths of 5-15 and 20-30 cm, all but a few sampling sites at the east and south boundaries had water available for use by plants.

REMOTELY SENSED SPECTRAL DATA

One means of obtaining regional information about the Earth's surface is with the use of remotely sensed data from satellites. Sensors similar to those in the satellites can be mounted and

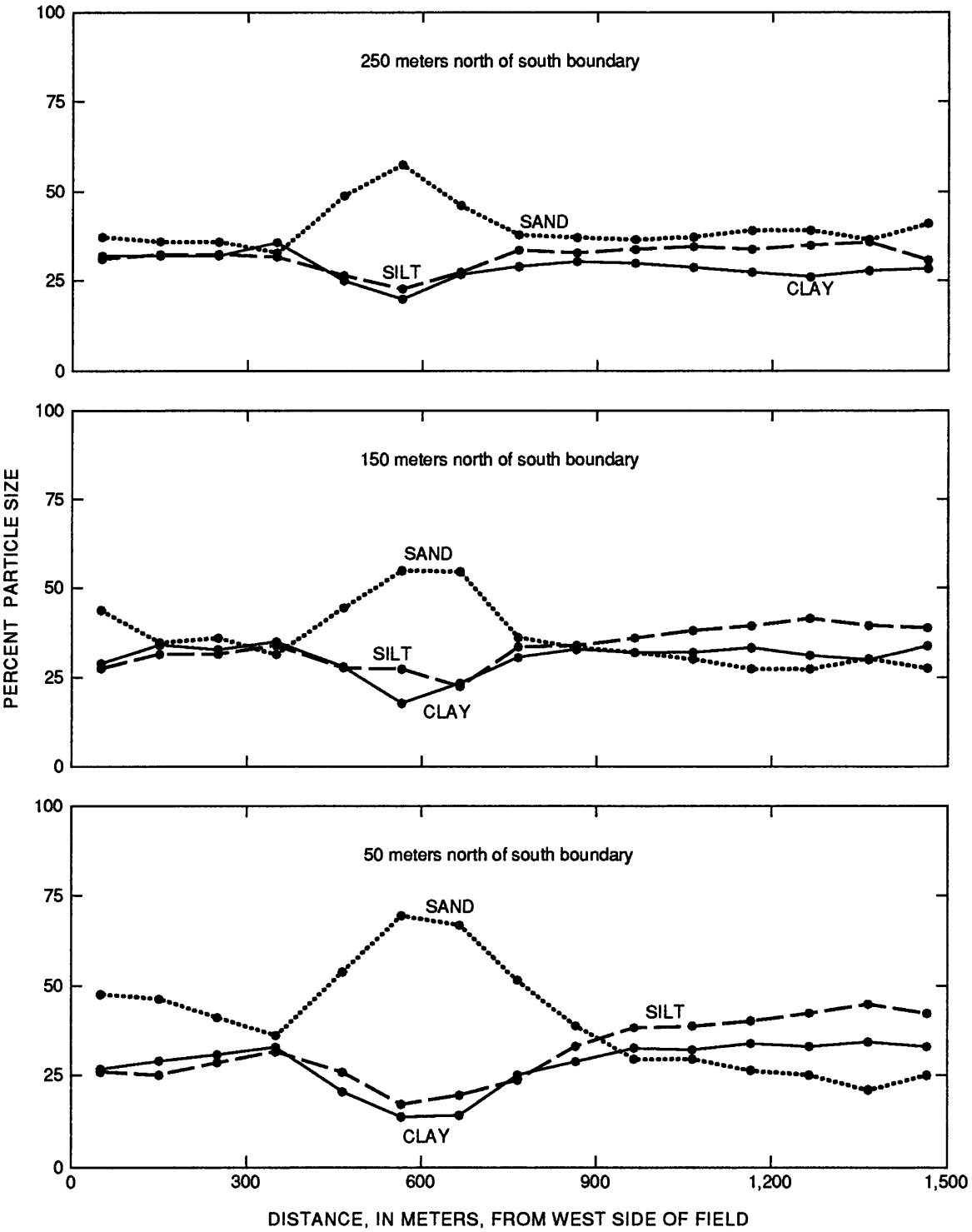

Figure 5.—Particle-size distribution (0-5 centimeters depth) along three east-west rows, 250, 150, and 50 meters north of the south boundary of field 28, Maricopa Agricultural Center.

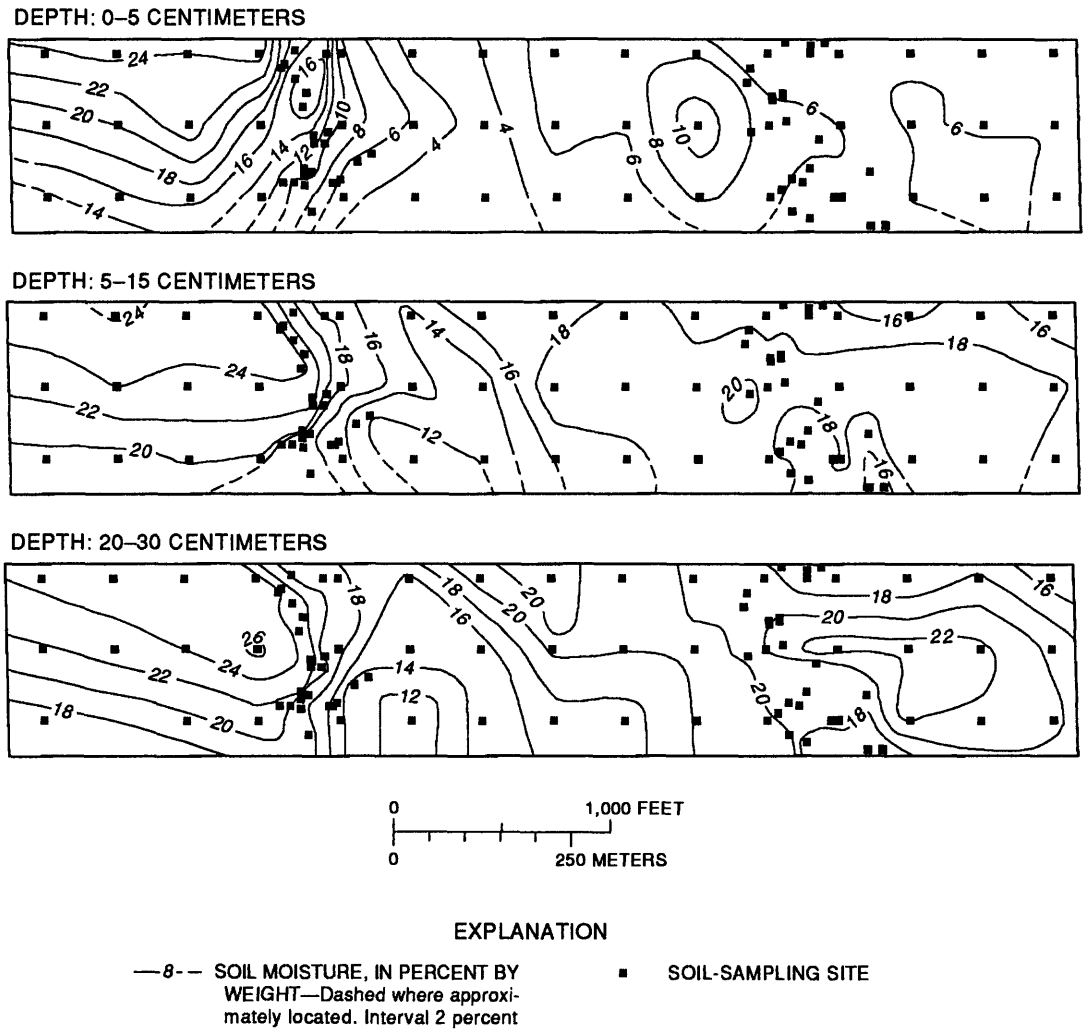

Figure 6.—Distribution of soil-moisture content measured the morning of day 164 at depths of 0–5, 5–15, and 20–30 centimeters in field 28, Maricopa Agricultural Center.

flown in aircraft to obtain data on a more local scale. In studies that require hourly or daily values to be calculated, one disadvantage of remotely sensed data is that the data provide only an instantaneous measure of the surface conditions.

Landsat Satellite

A Landsat thematic mapper (TM) scene was acquired on June 13, 1988 (day 165), to estimate the spatial variation in ET in field 28. The TM thermal data (band 6), required for estimating ET, were flawed by inexplicable horizontal stripes at regular intervals throughout the scene. Replacement tapes contained the same stripes. All attempts to remove the stripes resulted

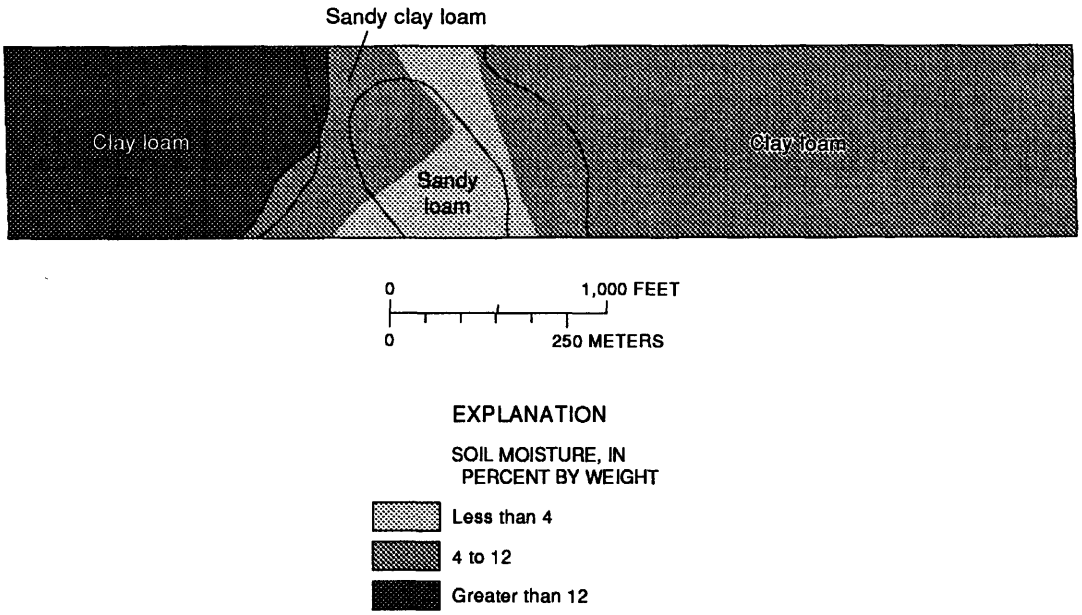

Figure 7.—Soil moisture (0–5 centimeters depth) measured the morning of day 164 overlaid on the soil textures (mapped by Post and others, 1988) in field 28, Maricopa Agricultural Center.

in data that were unusable to meet the needs of the project. Lack of the TM data prevented a full spatial comparison over the entire field.

Aircraft

A sensor package that simulates bands 1-4 and band 6 of the Landsat satellite thematic mapper was carried by light aircraft flying at an altitude of about 150 m over the fields. The aircraft flew the length of fields, and readings were taken at intervals along each flight line (fig. 9). Each flight line approximated the middle of the field as well as flight conditions allowed. Along each flight line, the number of readings depended on the speed of the aircraft. Each reading covered a circular area of ground about 40 m in diameter (pixel). A video camera operated continuously during the data acquisition; pixels were marked by a beep on the video sound track.

Aircraft data were available for one flight over field 28 on day 163 (figs. 10 and 11, table 1) and two flights on day 164 (figs. 10 and 11, table 2) (M. Susan Moran, Physical Scientist, U.S. Water Conservation Laboratory, written communs., 1988-90). Recognizable ground-control points were not included in the isolated pixels except for the first and last pixels near the field boundaries; therefore, the ground location of each pixel reading had to be estimated. The first and last pixels falling totally within the field boundaries were plotted in relation to ground positions seen on the video tape, and distances were measured by using the row spacing in the cotton field. When plotted, these flight lines through field 28 were not centrally located; the flight lines were about 40 m north of center, which corresponded more closely to the positions of the ground-based

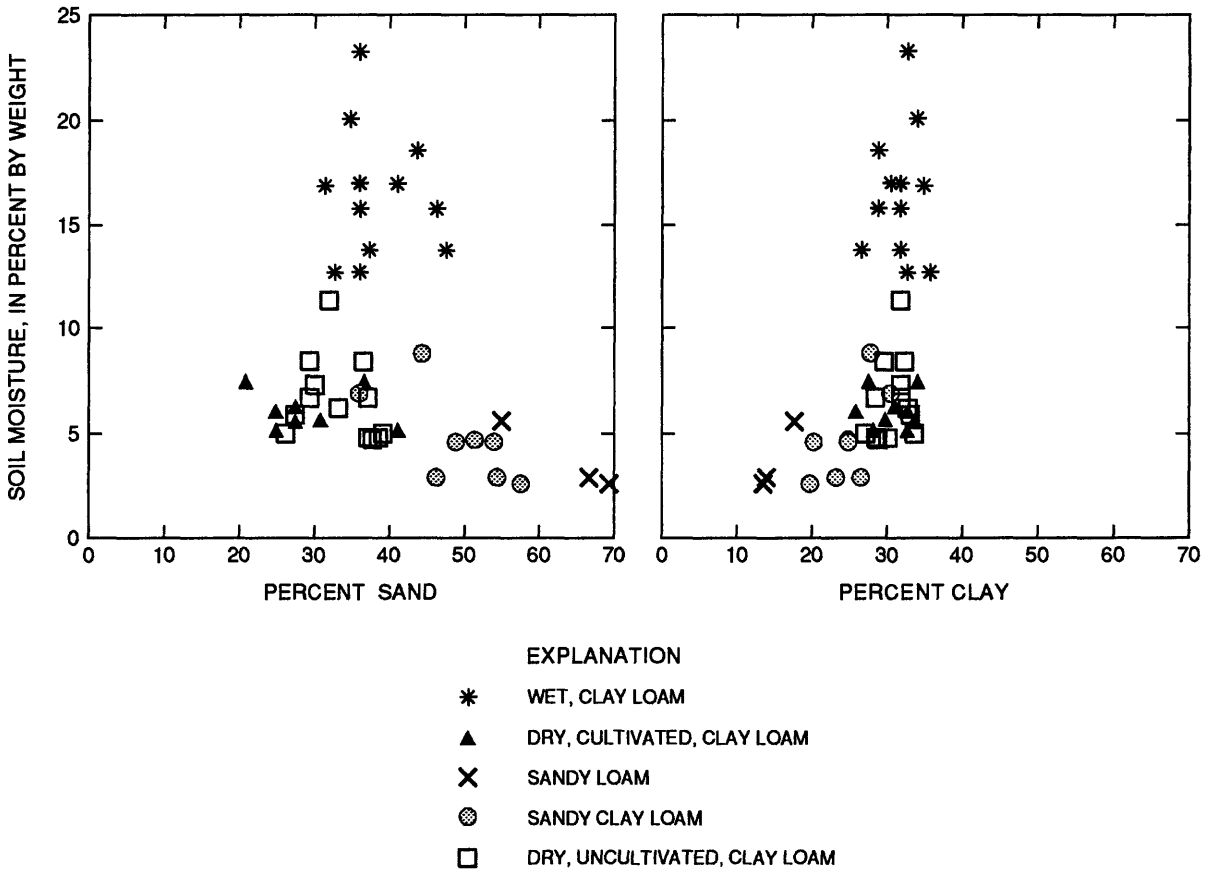

Figure 8.—Soil moisture (0–5 centimeters depth), percentages of sand and clay in the soil related to the soil textures (mapped by Post and others, 1988), and irrigation and cultivation characteristics on day 164 in field 28, Maricopa Agricultural Center.

scientific equipment. To map the data, a polygon coverage for each set of readings was created by (1) dividing the flight-line length between the first and last pixels plotted in the field by the number of aircraft readings between those two points, (2) calculating the UTM coordinates of the central point of each 40-m circle, and (3) generating a circle (ARC/INFO Users Manual, v. 1) with a 20-m radius (pixel) around each point (fig. 9).

An additional problem with locating the ground positions of the aircraft pixels was observed in the video tape. To compensate for wind, the plane was not oriented parallel to the flight line; to maintain the east-to-west line of flight, adjustments were made that resulted in shifts north and south along the flight line. These shifts were observed in the video tape but could not be considered when plotting pixel locations because of the lack of ground-control points in the field of view of the video camera.

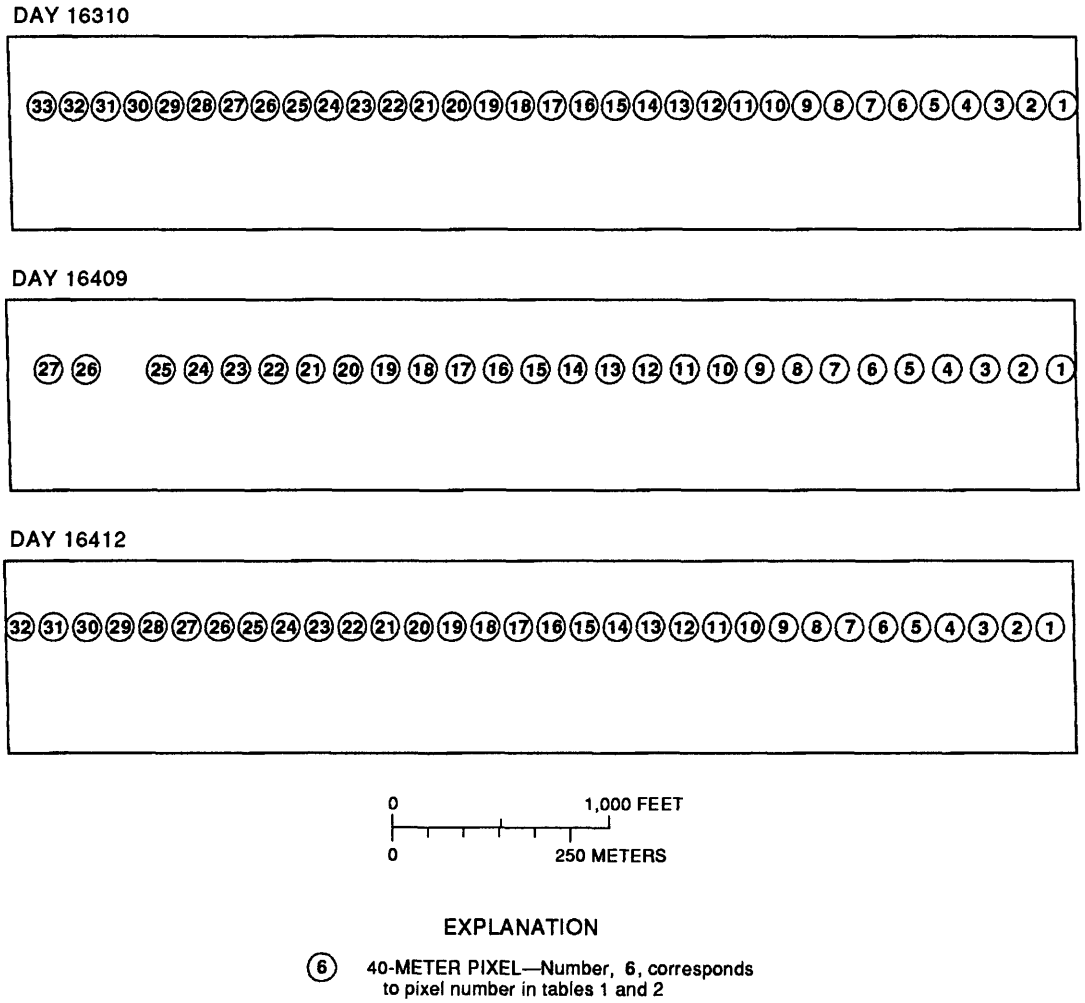

Figure 9.—Ground location of the 40-meter pixels that correspond to the readings from the aircraft-mounted sensor package that simulated bands 1–4 and 6 of the Landsat satellite thematic mapper along flight lines on day 163 at 1017 hours (16310) and on day 164 at 0911 (16409) and 1227 hours (16412) in field 28, Maricopa Agricultural Center.

EVAPOTRANSPIRATION

Remotely sensed measurements of reflected solar and emitted thermal (surface temperature) radiation combined with ground-based meteorological data—measurements of incoming solar radiation, air temperature, wind speed, and vapor pressure—have been used to calculate instantaneous ET (Jackson and others, 1987; Kustas and others, 1989). Mapping the spatial variability of ET over agricultural fields using remotely sensed data and an energy-balance equation has been demonstrated at MAC (Raymond and others, 1987, 1988; Moran and others, 1989).

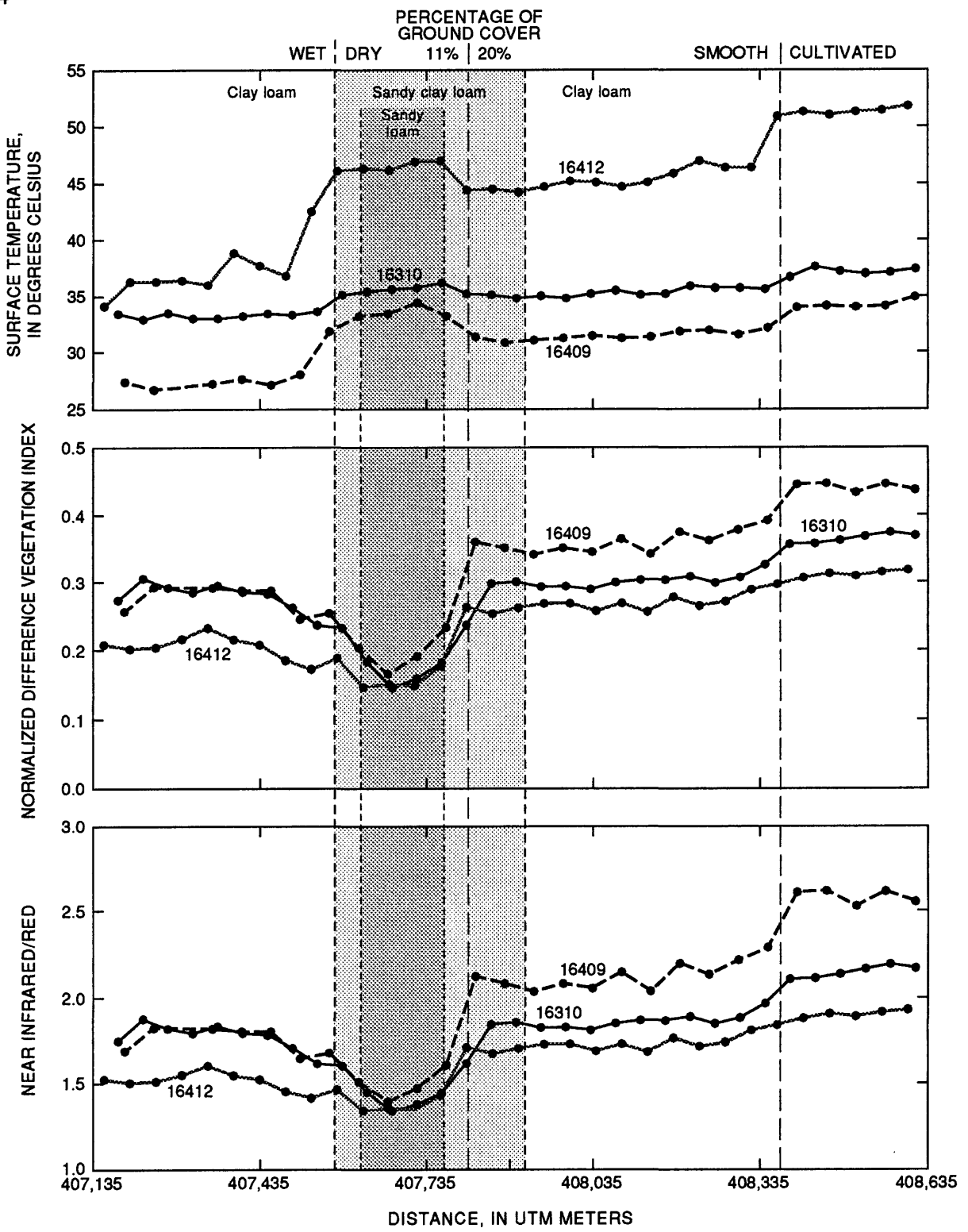

Figure 10.—Surface temperature, normalized difference vegetation index (NDVI), and near infrared (NIR)/red determined from remotely sensed aircraft data along flight lines on day 163 at 1017 hours (16310) and on day 164 at 0911 (16409) and 1227 hours (16412) in field 28, Maricopa Agricultural Center.

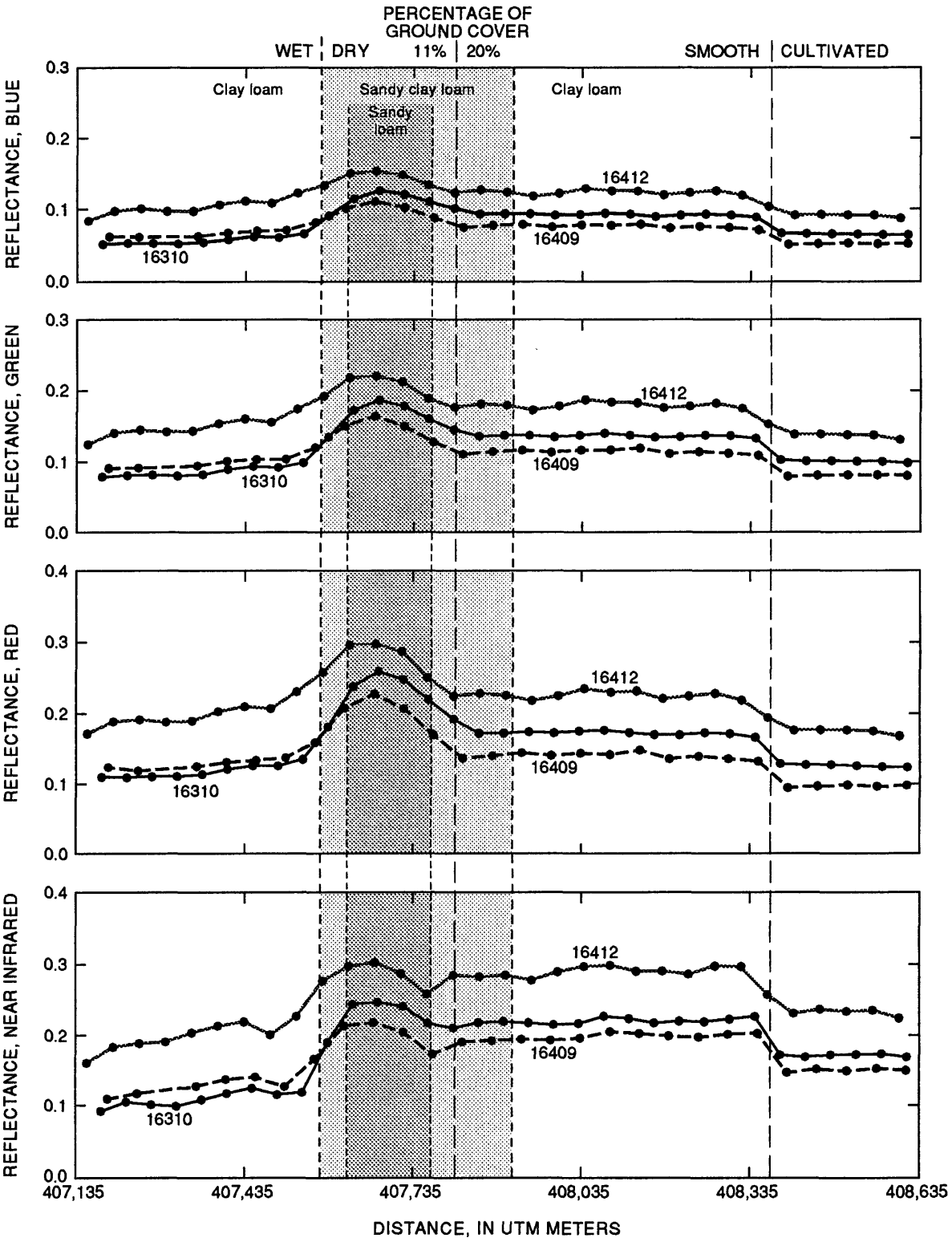

Figure 11.—Blue, green, red, and near infrared (NIR) reflectance determined from remotely sensed aircraft data along flight lines on day 163 at 1017 hours (16310) and on day 164 at 0911 (16409) and 1227 hours (16412) in field 28, Maricopa Agricultural Center.

Table 1.—*Aircraft-based surface-reflectance values collected over field 28 at the Maricopa Agricultural Center on June 11, 1988*

[TM, Thematic Mapper and band number; NIR, Near infrared; NDVI, Normalized Difference Vegetation Index; Temp., temperature; °C, degrees Celsius]

Pixel Number[1]	Hour	TM1 Blue	TM2 Green	TM3 Red	TM4 NIR	NIR/Red	NDVI	Temp. °C
1	10.2772	0.0640	0.0982	0.1239	0.2690	2.1709	0.3693	37.4
2	10.2775	0.0643	0.1002	0.1248	0.2738	2.1935	0.3737	37.1
3	10.2778	0.0651	0.1004	0.1259	0.2728	2.1665	0.3684	37.0
4	10.2781	0.0654	0.1012	0.1275	0.2724	2.1361	0.3623	37.2
5	10.2784	0.0657	0.1010	0.1275	0.2693	2.1124	0.3574	37.6
6	10.2787	0.0665	0.1026	0.1290	0.2719	2.1082	0.3565	36.7
7	10.2790	0.0887	0.1329	0.1661	0.3267	1.9668	0.3259	35.6
8	10.2793	0.0916	0.1368	0.1713	0.3229	1.8848	0.3067	35.7
9	10.2796	0.0926	0.1373	0.1727	0.3196	1.8510	0.2985	35.7
10	10.2798	0.0913	0.1350	0.1695	0.3203	1.8896	0.3079	35.9
11	10.2801	0.0895	0.1343	0.1700	0.3176	1.8688	0.3028	35.2
12	10.2804	0.0928	0.1373	0.1730	0.3235	1.8698	0.3031	35.1
13	10.2807	0.0940	0.1401	0.1764	0.3270	1.8541	0.2993	35.5
14	10.2810	0.0924	0.1374	0.1750	0.3171	1.8120	0.2888	35.2
15	10.2813	0.0913	0.1348	0.1723	0.3153	1.8297	0.2932	34.8
16	10.2816	0.0934	0.1371	0.1739	0.3177	1.8267	0.2925	35.0
17	10.2819	0.0934	0.1371	0.1722	0.3198	1.8577	0.3001	34.8
18	10.2822	0.0930	0.1359	0.1722	0.3181	1.8468	0.2974	35.1
19	10.2825	0.1005	0.1450	0.1921	0.3105	1.6168	0.2357	35.2
20	10.2828	0.1105	0.1604	0.2198	0.3172	1.4434	0.1815	36.2
21	10.2831	0.1208	0.1786	0.2475	0.3413	1.3791	0.1593	35.7
22	10.2834	0.1263	0.1866	0.2591	0.3472	1.3398	0.1452	35.6
23	10.2837	0.1148	0.1728	0.2379	0.3442	1.4470	0.1827	35.4
24	10.2840	0.0905	0.1347	0.1809	0.2899	1.6025	0.2315	35.1
25	10.2843	0.0655	0.0985	0.1351	0.2183	1.6159	0.2355	33.6
26	10.2846	0.0607	0.0922	0.1261	0.2152	1.7072	0.2612	33.3
27	10.2849	0.0618	0.0937	0.1260	0.2247	1.7836	0.2815	33.4
28	10.2852	0.0578	0.0891	0.1208	0.2169	1.7948	0.2844	33.2
29	10.2855	0.0538	0.0820	0.1135	0.2081	1.8342	0.2943	33.0
30	10.2858	0.0517	0.0803	0.1110	0.1990	1.7935	0.2840	33.0
31	10.2861	0.0524	0.0817	0.1105	0.2012	1.8212	0.2911	33.5
32	10.2864	0.0527	0.0808	0.1091	0.2048	1.8773	0.3049	32.9
33	10.2867	0.0510	0.0787	0.1099	0.1921	1.7480	0.2722	33.4

[1]Corresponds to pixel locations plotted on figure 8.

Table 2.—*Aircraft-based surface-reflectance values collected over field 28 at the Maricopa Agricultural Center on June 12, 1988*

[TM, Thematic Mapper and band number; NIR, Near infrared; NDVI, Normalized Difference Vegetation Index; Temp., temperature; °C, degrees Celsius]

Pixel Number[1]	Hour	TM1 Blue	TM2 Green	TM3 Red	TM4 NIR	NIR/Red	NDVI	Temp. °C
				Early Morning Flight				
1	9.1864	0.0518	0.0803	0.0979	0.2500	2.5531	0.4371	34.9
2	9.1867	0.0516	0.0813	0.0968	0.2528	2.6127	0.4464	34.1
3	9.1870	0.0527	0.0815	0.0987	0.2496	2.5292	0.4333	34.0
4	9.1873	0.0516	0.0812	0.0965	0.2523	2.6154	0.4468	34.1
5	9.1876	0.0509	0.0790	0.0949	0.2473	2.6066	0.4455	34.0
6	9.1879	0.0712	0.1090	0.1323	0.3027	2.2883	0.3918	32.1
7	9.1882	0.0744	0.1118	0.1361	0.3016	2.2164	0.3782	31.5
8	9.1885	0.0757	0.1140	0.1395	0.2977	2.1345	0.3619	31.9
9	9.1888	0.0735	0.1112	0.1361	0.2991	2.1983	0.3747	31.8
10	9.1891	0.0788	0.1192	0.1484	0.3025	2.0384	0.3418	31.3
11	9.1894	0.0771	0.1167	0.1422	0.3055	2.1486	0.3648	31.2
12	9.1897	0.0777	0.1164	0.1441	0.2962	2.0553	0.3454	31.4
13	9.1900	0.0749	0.1133	0.1408	0.2933	2.0827	0.3512	31.2
14	9.1903	0.0786	0.1164	0.1446	0.2945	2.0363	0.3413	31.0
15	9.1905	0.0775	0.1143	0.1405	0.2927	2.0825	0.3512	30.8
16	9.1908	0.0743	0.1107	0.1369	0.2909	2.1253	0.3601	31.3
17	9.1911	0.0877	0.1275	0.1702	0.2734	1.6061	0.2326	33.2
18	9.1914	0.1021	0.1501	0.2070	0.3047	1.4715	0.1908	34.4
19	9.1917	0.1109	0.1643	0.2280	0.3185	1.3967	0.1655	33.4
20	9.1920	0.1011	0.1507	0.2078	0.3136	1.5089	0.2028	33.2
21	9.1923	0.0814	0.1200	0.1588	0.2666	1.6786	0.2533	31.8
22	9.1926	0.0705	0.1036	0.1376	0.2265	1.6454	0.2440	28.0
23	9.1929	0.0696	0.1032	0.1335	0.2408	1.8043	0.2868	27.1
24	9.1932	0.0669	0.1007	0.1312	0.2370	1.8059	0.2872	27.6
25	9.1935	0.0623	0.0942	0.1250	0.2274	1.8198	0.2907	27.2
26	9.1941	0.0614	0.0913	0.1188	0.2168	1.8248	0.2920	26.7
27	9.1944	0.0618	0.0906	0.1238	0.2092	1.6898	0.2565	27.4
				Midday Flight				
1	12.4472	0.0871	0.1307	0.1680	0.3243	1.9309	0.3176	51.8
2	12.4475	0.0915	0.1374	0.1750	0.3357	1.9186	0.3147	51.4

Table 2.—*Aircraft-based surface-reflectance values collected over field 28 at the Maricopa Agricultural Center on June 12, 1988*—Continued

[TM, Thematic Mapper and band number; NIR, Near infrared; NDVI, Normalized Difference Vegetation Index; Temp., temperature; °C, degrees Celsius]

Pixel Number[1]	Hour	TM1 Blue	TM2 Green	TM3 Red	TM4 NIR	NIR/Red	NDVI	Temp. °C
				Midday Flight—Continued				
3	12.4478	0.0918	0.1378	0.1764	0.3339	1.8926	0.3086	51.3
4	12.4481	0.0924	0.1387	0.1766	0.3371	1.9088	0.3124	51.0
5	12.4484	0.0914	0.1385	0.1760	0.3312	1.8813	0.3059	51.3
6	12.4487	0.1033	0.1532	0.1943	0.3579	1.8417	0.2962	50.9
7	12.4490	0.1194	0.1752	0.2192	0.3969	1.8106	0.2884	46.4
8	12.4493	0.1257	0.1823	0.2285	0.3978	1.7411	0.2704	46.4
9	12.4496	0.1232	0.1786	0.2248	0.3861	1.7177	0.2641	47.0
10	12.4499	0.1200	0.1761	0.2212	0.3908	1.7665	0.2771	45.9
11	12.4502	0.1251	0.1829	0.2317	0.3904	1.6849	0.2551	45.1
12	12.4505	0.1257	0.1840	0.2302	0.3988	1.7319	0.2679	44.7
13	12.4508	0.1289	0.1873	0.2350	0.3971	1.6901	0.2565	45.1
14	12.4511	0.1220	0.1784	0.2252	0.3896	1.7304	0.2675	45.2
15	12.4514	0.1184	0.1729	0.2184	0.3777	1.7294	0.2672	44.7
16	12.4517	0.1238	0.1795	0.2258	0.3852	1.7059	0.2609	44.2
17	12.4520	0.1270	0.1816	0.2286	0.3829	1.6752	0.2524	44.5
18	12.4523	0.1228	0.1769	0.2248	0.3847	1.7116	0.2624	44.4
19	12.4526	0.1339	0.1893	0.2507	0.3585	1.4297	0.1769	47.0
20	12.4529	0.1483	0.2120	0.2870	0.3871	1.3485	0.1484	46.9
21	12.4532	0.1533	0.2198	0.2974	0.4029	1.3548	0.1507	46.2
22	12.4535	0.1506	0.2177	0.2959	0.3973	1.3429	0.1463	46.3
23	12.4538	0.1335	0.1925	0.2574	0.3767	1.4637	0.1882	46.1
24	12.4541	0.1226	0.1742	0.2310	0.3269	1.4154	0.1720	42.5
25	12.4543	0.1085	0.1558	0.2071	0.3009	1.4532	0.1847	36.8
26	12.4546	0.1114	0.1605	0.2099	0.3195	1.5223	0.2071	37.7
27	12.4549	0.1063	0.1539	0.2027	0.3134	1.5460	0.2145	38.8
28	12.4552	0.0973	0.1433	0.1894	0.3036	1.6025	0.2315	36.0
29	12.4555	0.0973	0.1422	0.1878	0.2908	1.5488	0.2153	36.4
30	12.4558	0.1010	0.1448	0.1910	0.2885	1.5106	0.2034	36.3
31	12.4561	0.0973	0.1404	0.1885	0.2835	1.5039	0.2013	36.3
32	12.4564	0.0834	0.1243	0.1712	0.2608	1.5234	0.2074	34.1

[1]Corresponds to pixel locations plotted on figure 8.

Calculation of instantaneous ET depends on the relation among the components in the energy balance for a surface. The energy-balance equation used by Jackson and others (1987) is

$$LE = R_n - G - H, \tag{1}$$

where *LE*, latent heat flux density, is the rate of energy utilized in ET (a product of the heat of vaporization, *L*, and the rate of evaporation, *E*), R_n is the net radiant flux density, *G* is the soil heat flux density, and *H* is sensible heat flux density. R_n is the sum of incoming and outgoing radiant flux densities and is expressed as

$$R_n = R_{L\downarrow} + R_{S\downarrow} - R_{L\uparrow} - R_{S\uparrow}, \tag{2}$$

where $R_{L\downarrow}$ and $R_{S\downarrow}$ are incoming long- (> 4 μm) and short-wave (0.15 to 4 μm) radiation falling on ground and plant surfaces, and $R_{L\uparrow}$ and $R_{S\uparrow}$ are emitted and reflected long- and short-wave radiation from ground and plant surfaces. All terms are in W/m^2. $R_{L\downarrow}$ is estimated from ground-based measurements of air temperature and vapor pressure, and $R_{S\downarrow}$ is measured directly with a calibrated pyranometer. $R_{L\uparrow}$ and $R_{S\uparrow}$ are calculated from data collected by a four-band—blue, green, red, and near infrared (NIR)—multispectral radiometer and a single-band thermal infrared (IR) thermometer carried aboard light aircraft. $R_{S\uparrow}$ is corrected for atmospheric absorption and scattering by using a radiative transfer model (Jackson, 1984). Soil heat flux is determined by a relation between *G* and R_n as

$$G/R_n = 0.583\, e^{-2.13NDVI}, \tag{3}$$

where *NDVI* is the normalized difference vegetation index [(NIR - red)/(NIR + red)]. Sensible heat flux is estimated from the difference between surface temperature and air temperature and a stability-corrected aerodynamic resistance that is a function of surface and air temperatures, wind speed, height above the surface at which wind speed and air temperature are measured, and the aerodynamic parameters of surface roughness and displacement. Sensible heat flux is calculated as

$$H = \rho C_p (T_s - T_a)/r_a, \tag{4}$$

where ρC_p is the volumetric heat capacity, T_s is the surface temperature, T_a is the air temperature, and r_a is the aerodynamic resistance. The value for r_a is determined using the formula of Mahrt and Ek (1984):

for $(T_s - T_a) < 0$ (stable)

$$r_a = \{\ln[(z-d+z_o)/z_o]/k\}^2 (1+15Ri)(1+5Ri)^{1/2}/U, \tag{5}$$

for $(T_s - T_a) > 0$ (unstable)

$$r_a = \{\ln[(z-d+z_o)/z_o]/k\}^2\{1-15Ri/[1+C(-Ri)^{1/2}]\}^{-1}/U, \quad (6)$$

where z is the height above the ground surface at which windspeed (U) and T_a are measured; d is the displacement height; z_o is the surface roughness; k is von Karman's constant (0.4); Ri is the Richardson number calculated as

$$Ri = g(T_a - T_s)(z-d)/T_a U^2, \quad (7)$$

where g is the acceleration due to gravity; and

$$C = 75k^2[(z-d+z_o)/z_o]^{1/2}/\{\ln[(z-d+z_o)/z_o]\}^2. \quad (8)$$

In this analysis to more closely represent actual meteorological conditions for the energy balance, a running average was applied to the instantaneous (15-second) data collected by the meteorological station. *LE* was computed by temporally matching a set of instantaneous spectral surface-reflectance data (tables 1 and 2) with averaged meteorological data that bracketed a 15-minute period around the time of the spectral-data acquisition. Averaging eliminated anomalous values, such as wind gusts, from the data.

Jackson and others (1987) showed that estimating *LE* from remotely sensed data works best when the agricultural fields are large, uniform, and in full cover. In this previous study, the aircraft-based technique detected significant differences in *LE* because of differences in irrigation and crop density. Research continues in testing the method over partial-canopy conditions. If this method is to have application in estimating water use beyond short-term estimates used in research, then the difficulties encountered over partial canopies need to be resolved.

Remotely sensed measurements of emitted thermal radiation (T_s) are required to estimate H (equations 4 and 7). Nadir-looking airborne sensors give composite readings over the field of view of the sensor. Of particular concern to using remotely sensed data to estimate ET is the composite T_s given by the IR sensor. In fields with less than full cover, the IR sensor measures a composite T_s of the plants, soil, and shaded surfaces. The remote method proposed to estimate *LE* does not work in partial-canopy situations (Ray D. Jackson, Research Physicist, U.S. Water Conservation Laboratory, written commun., 1991). In the case of field 28 in June 1988, the measured T_s is dominated by the hot soil surface rather than the transpiring plants and use of these temperatures does not provide adequate estimates of *LE* when using the remote method.

Because estimates of *LE* cannot be determined and related to soil moisture for this study, the values of T_s were spatially related to soil moisture to illustrate the partial-canopy problem. A graph of the composite T_s (TM band 6) at each pixel along the three flight lines (fig. 10) shows that the values easily group into ranges of 10°C that correspond to the changes in surface conditions. Low values of T_s, less than 40°C, were associated with recent irrigation in the west 400 m of field 28. High values, greater than 40°C, corresponded to dry conditions in the east 1,100 m; values greater than 50°C corresponded to the cultivated area. Along all three flight lines, T_s showed similar trends from pixel to pixel, although the magnitude of change was less pronounced

on day 163 (fig. 10). Changes from one trend to another delineated the wet from dry, the smooth from cultivated in the Trix clay loam, and the sandy loam from sandy clay loam and were common to flights on both days. The most predominant change between the wet and dry parts of the field was common to all the data sets (figs. 10 and 11), although the position of the change appeared to be moving west with time because of drying. The surface soils dry quickly under hot, dry desert conditions. To map the data spatially, shading patterns were selected and plotted for the generated pixels and overlaid on maps of soil textures (fig. 12) and soil moisture at 0-5 cm (fig. 13). Changes in T_s did not correspond to changes in soil texture (fig. 12) but did indicate wet, >16 percent, as opposed to dry soil moisture and cultivated as opposed to smooth surface roughness (fig. 13).

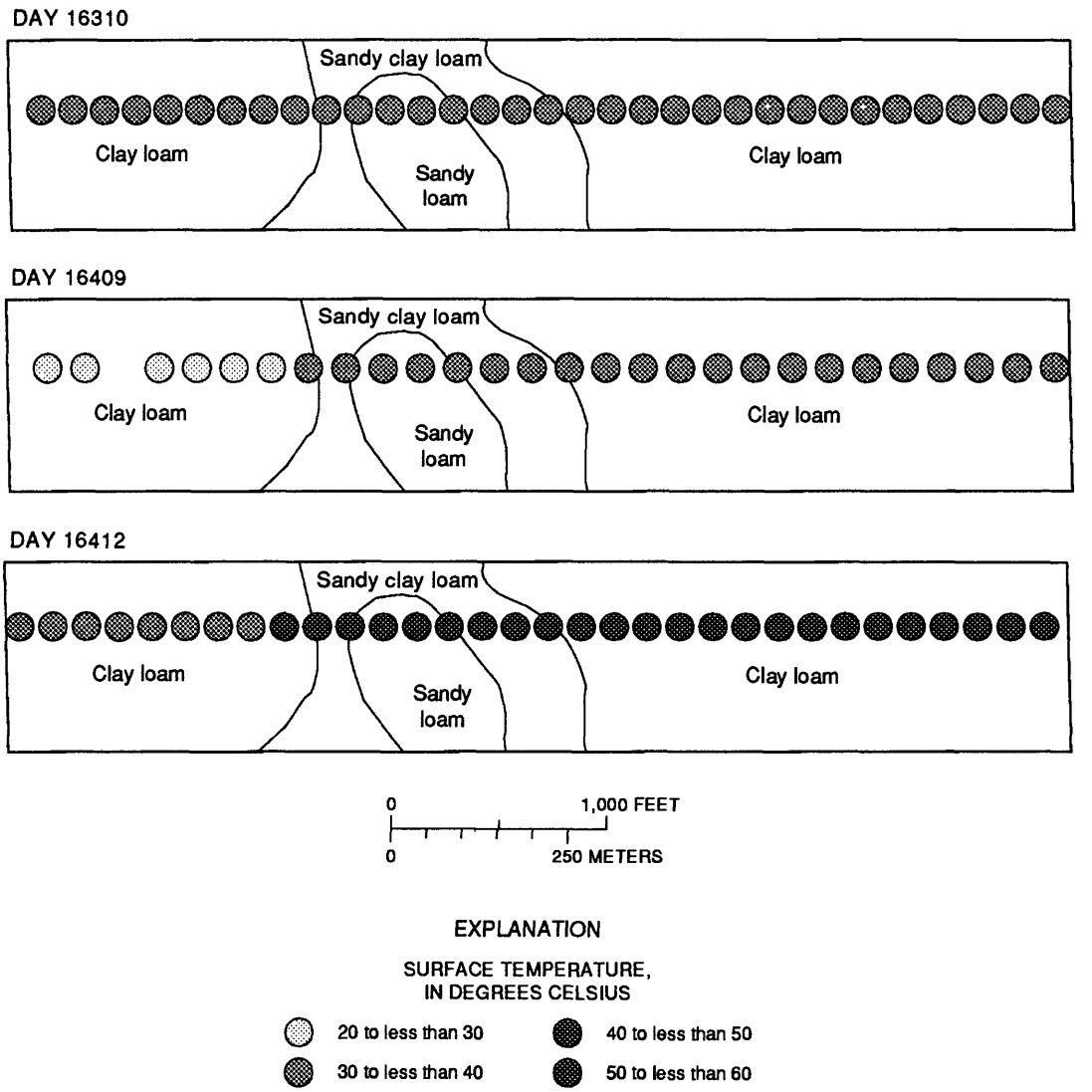

Figure 12.—Remotely sensed surface temperature shown spatially along flight lines on day 163 at 1017 hours (16310) and on day 164 at 0911 (16409) and 1227 hours (16412) overlaid on the soil textures (mapped by Post and others, 1988) in field 28, Maricopa Agricultural Center.

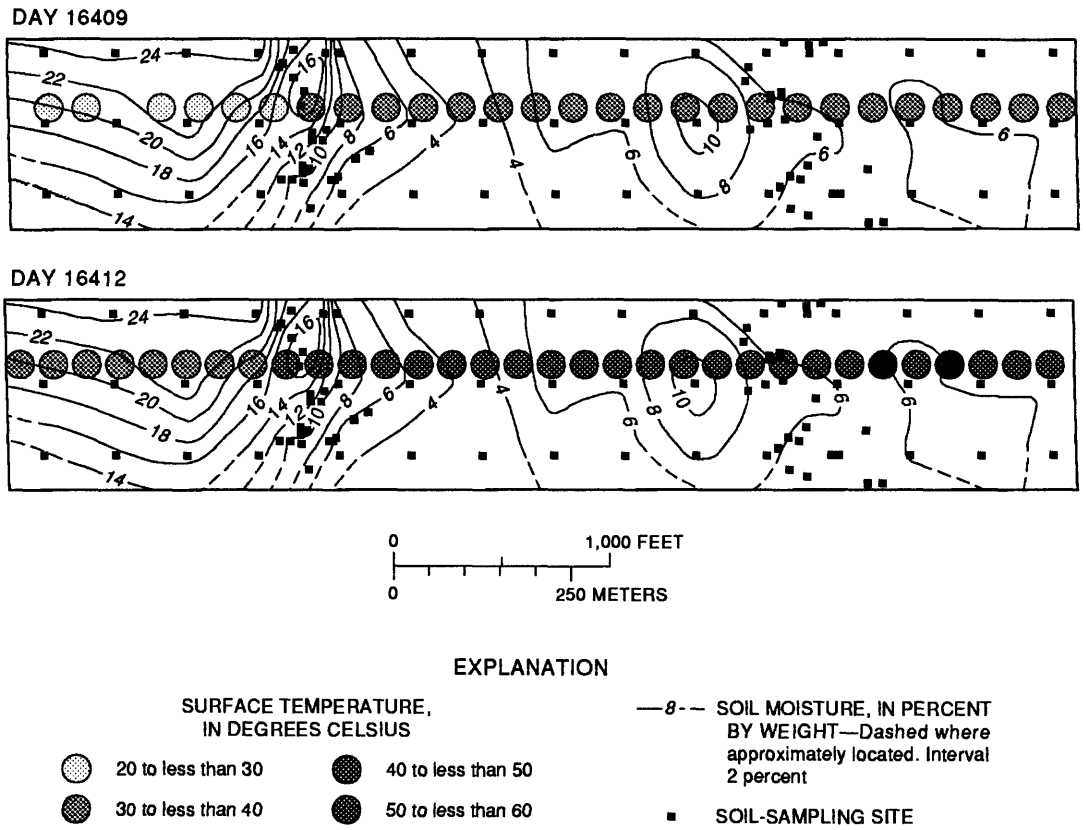

Figure 13.—Remotely sensed surface temperature shown spatially along flight lines on day 164 at 0911 (16409) and 1227 hours (16412) overlaid on the soil moisture measured the morning of day 164 in field 28, Maricopa Agricultural Center.

Changes in T_s were affected more by changes in the soil surface, which mask any change caused by the difference in ground cover.

Average values of soil moisture at a sampling depth of 0-5 cm were estimated from the contour map at points corresponding to the 40-m pixels for which T_s estimates were made. Plotting the relation between T_s and soil moisture resulted in two populations of data points—those in the wet area and those in the dry area (fig. 14A at 0911 hours; fig. 14B at 1227 hours). Data points also were coded to show roughness, which resulted in two populations, smooth and cultivated. Data points in the cultivated area separated from the points over smooth surfaces in the dry group as the temperatures increased at midday. For data points in each of the groups, T_s varied less than soil moisture (fig. 14). The larger range in T_s values for the wet population near midday was caused by surface drying; some points were in transition to the dry population at 1227 hours (fig. 14B).

Remotely sensed measurements of reflected solar radiation in the NIR and red bands are used to calculate *NDVI* for input into the estimate of G (equation 3). *NDVI* is a spectral index that estimates the amount of vegetation present; therefore, two *NDVI* responses should result from two

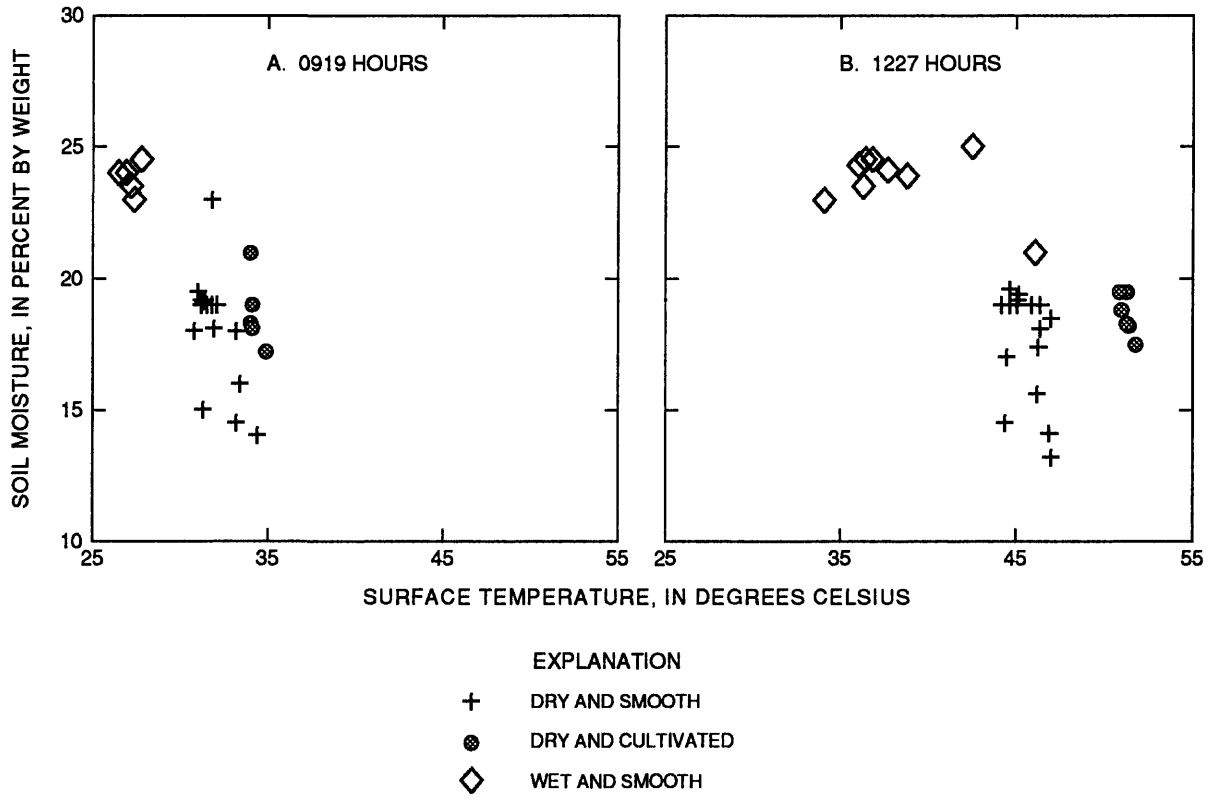

Figure 14.—Soil moisture (0–5 centimeters depth) measured on day 164 and remotely sensed surface temperature on day 164 in field 28, Maricopa Agricultural Center.

different canopy densities. Instead, the *NDVI* response was more sensitive to variations in the underlying soils than to the change in canopy density (fig. 10). Huete and Warrick (1990) used the soil-moisture data in combination with aircraft-reflectance data obtained using the SPOT filters on the radiometer (flights on day 163 at 1133 hours and day 164 at 1113 hours) to investigate estimating soil moisture using canopy thermal and brightness responses. Huete and Warrick (1990) found that the spatial and temporal dynamics of soil-surface drying and roughness differences resulting from cultivation altered the *NDVI* responses over large-size pixel measurements obtained from aerial and satellite platforms.

Most investigations into estimating ET for partial canopies collected data over sparse rangeland vegetation in arid regions. Under arid conditions and sparse vegetation as in Owens Valley, California, Kustas and others (1989) found that equations 4 and 5 could not provide appropriate values of r_a and therefore lead to unsatisfactory values of H. To obtain appropriate values of r_a, Kustas and others (1989) allowed the resistance to heat transfer, kB^{-1}, to vary and showed that for partial canopy under arid conditions kB^{-1} may be a function of T_s measured

radiometrically. Moran and others (1991) applied the kB^{-1} equation and another method of defining a resistance term that is independent of aerodynamic resistance and related only to soil-surface temperature to data collected over sparse rangeland vegetation near Tombstone, Arizona. Kustas and others (1989) and Moran and others (1991) stated that further work is required on many of the components of the remote method of estimating *LE*. Although estimates of remote *LE* were the same magnitude and trend as ground-based measurements, differences at times were significant and time of day and clear sky conditions imposed serious limitations to the method (Moran and others, 1991).

Ground-based experimental studies for sparse vegetation attempt to solve the energy budget by separating the canopy and underlying soil. A study over sparse cotton by Ham and Heilman (1991) supports the theory that simple gradient diffusion models that use standard micrometeorological data cannot be used to predict flux within the canopy. Experimental studies that examine factors affecting energy transport from the soil and canopy separately should help to overcome the inability to quantify aerodynamic transport within sparse vegetation. A similar study over sparse rangeland vegetation by Nichols (1992) supported conclusions by Ham and Heilman (1991), but further studies are needed of the factors controlling canopy and aerodynamic resistances.

SUMMARY

Remotely sensed spectral data collected from an aircraft platform were compared to gravimetric soil-moisture content in field 28 of the Maricopa Agricultural Center. Data were plotted graphically along flight lines and sampling rows and were mapped to show spatial comparisons using geographic information system (GIS) software. Soil moisture did not vary as a function of soil texture or surface roughness. Surface temperature measured by the infrared sensor is the remotely sensed component of the remote method of estimating evapotranspiration, but under partial-canopy conditions, surface temperature is a composite of the plants, soil, and shaded surfaces within the sensor field of view. Under field conditions that existed during data collection in June 1988, the hot soil surface dominated the composite surface temperature. The high composite surface temperatures resulted in calculated values of sensible heat flux that were too large, and therefore latent heat flux was negligible, even though the plants were transpiring. Changes in surface temperature correlated with changes in surface roughness, cultivated as opposed to smooth soil, and with soil moisture, wet as opposed to dry. Changes in soil surface masked any change caused by the difference in ground cover. Ground-based studies continue to attempt to solve separate soil and canopy energy budgets in order to quantify aerodynamic transport with sparse vegetation.

GIS software provides the ability to rigorously compare sets of spatial data, but the accuracy of positioning in each spatial data set becomes important to the comparison process. Inaccuracies in the positioning of spatial data points transfer directly into any spatial comparisons, which can result in a misrepresentation of relations between mapped variables. Finding a means by which the data collected from an aircraft can be accurately positioned on the ground is necessary to enhance its use in GIS data analysis.

REFERENCES

ARC/INFO Users Manual, Version 5, 1989: Environmental Systems Research Institute, Redlands, California.

Daughtry, C.S.T., Kustas, W.P., Moran, M.S., Pinter, P.J., Jr., Jackson, R.D., Brown, P.W., Nichols, W.D., and Gay, L.W., 1990, Spectral estimates of net radiation and soil heat flux: Remote Sensing of Environment, v. 32, p. 111-124.

Ham, J.M., and Heilman, J.L., 1991, Aerodynamic and surface resistances affecting energy transport in a sparse crop: Agricultural and Forest Meteorology, v. 53, p. 267-284.

Huete, A.R., and Warrick, A.W., 1990, Assessment of vegetation and soil water regimes in partial canopies with optical remotely sensed data: Remote Sensing of Environment, v. 32, p. 155-167.

Jackson, R.D., 1984, Total reflected solar radiation calculated from multi-band sensor data: Agricultural and Forest Meteorology, v. 33, p. 164-175.

Jackson, R.D., Hatfield, J.L., Reginato, R.J., Idso, S.B., and Pinter, P.J., Jr., 1983, Estimation of daily evapotranspiration from one time-of-day measurements: Agricultural Water Management, v. 7, p. 351-362.

Jackson, R.D., Moran, M.S., Gay, L.W., and Raymond, L.H., 1987, Evaluating evaporation from field crops using airborne radiometry and ground-based meteorological data: Irrigation Science, v. 8, p. 81-90.

Kustas, W.P., Choudhury, B.J., Moran, M.S., Reginato, R.J., Jackson, R.D., Gay, L.W., Weaver, H.L., 1989, Determination of sensible heat flux over sparse canopy using thermal infrared data: Agricultural and Forest Meteorology, v. 44, p. 197-216.

Kustas, W.P., Jackson, R.D., and Asrar, Ghassem, 1989, Estimating surface energy-balance components from remotely sensed data, *in* Asrar, Ghassem, ed., Theory and Applications of Optical Remote Sensing: New York, John Wiley, p. 604-627.

Moran, M.S., 1986a, The MAC experiment: The University of Arizona Remote Sensing Newsletter, v. 86-1, p. 1-4.

_____1986b, The MAC experiment—a cooperative research project in agricultural remote sensing: Conference on Remote Sensing and Geographic Information Systems in Management, Tucson, Arizona, November 6-7, 1986, Proceedings, p. 66-72.

Moran, M.S., Jackson, R.D., Raymond, L.H., Gay, L.W., and Slater, P.N., 1989, Mapping surface energy balance components by combining Landsat Thematic Mapper and ground-based meteorological data: Remote Sensing of Environment, v. 30, p. 77-87.

Moran, M.S., Kustas, W.P., Vidal, Alain, Stannard, D.I., and Blanford, James, 1991, Use of ground-based remotely sensed data for surface energy balance calculations during Monsoon '90: International Geoscience and Remote Sensing Symposium 1991 (IGARSS'91), Espoo, Finland, June 3-6, 1991, Proceedings, p. 33-37.

Nichols, W.D., 1992, Energy budgets and resistances to energy transport in sparsely vegetated rangeland: Agricultural and Forest Meteorology, v. 60, nos. 3 and 4, p. 221-247.

Post, D.F., Mack, Chris, Camp, P.D., and Suliman, A.S., 1988, Mapping and characterization of the soils on the University of Arizona Maricopa Agricultural Center: Hydrology and Water Resources in Arizona and the Southwest, Arizona-Nevada Academy of Science, v. 18, Proceedings, p. 49-60.

Raymond, L.H., Moran, M.S., and Jackson, R.D., 1987, Mapping latent heat energy from remotely sensed data and other variables using geographic information system software: Conference on Spatial Data Systems for Management, Tucson, Arizona, November 5-6, 1987, Proceedings, p. 38-45.

_____1988, Mapping evapotranspiration using the energy-budget method with remotely sensed data: Symposium on Water-Use Data for Water Resources Management, American Water Resources Association, Tucson, Arizona, August 29-31, 1988, Proceedings, p. 655-665.

Regan, J.J., Post, D.F., and Rauschkolb, R.S., 1989, Mapping the Maricopa Agricultural Center using a geographic information system: Hydrology and Water Resources in Arizona and the Southwest, Arizona-Nevada Academy of Science, v. 19, Proceedings, p. 47-58.